

**Zeitschrift:** Helvetica Physica Acta  
**Band:** 56 (1983)  
**Heft:** 1-3

**Artikel:** Applications of superlattices  
**Autor:** Linh, Nuyen T.  
**DOI:** <https://doi.org/10.5169/seals-115383>

### **Nutzungsbedingungen**

Die ETH-Bibliothek ist die Anbieterin der digitalisierten Zeitschriften. Sie besitzt keine Urheberrechte an den Zeitschriften und ist nicht verantwortlich für deren Inhalte. Die Rechte liegen in der Regel bei den Herausgebern beziehungsweise den externen Rechteinhabern. [Siehe Rechtliche Hinweise.](#)

### **Conditions d'utilisation**

L'ETH Library est le fournisseur des revues numérisées. Elle ne détient aucun droit d'auteur sur les revues et n'est pas responsable de leur contenu. En règle générale, les droits sont détenus par les éditeurs ou les détenteurs de droits externes. [Voir Informations légales.](#)

### **Terms of use**

The ETH Library is the provider of the digitised journals. It does not own any copyrights to the journals and is not responsible for their content. The rights usually lie with the publishers or the external rights holders. [See Legal notice.](#)

**Download PDF:** 22.05.2025

**ETH-Bibliothek Zürich, E-Periodica, <https://www.e-periodica.ch>**

## APPLICATIONS OF SUPERLATTICES

NUYEN T. LINH

Thomson-CSF Central Research Laboratory  
Domaine de Corbeville 91401 Orsay France

### Abstract.

Since the first work on periodic superlattice, many studies have been devoted to heterojunction multilayers. Combinations of different material properties have led to a new class of semiconductors exhibiting interesting electronic properties. Applications in the field of quantum well lasers, two-dimensional electron gas field effect transistors, superlattice avalanche photo-diode... are described. Conclusion is given on the tight cooperation between physicists and engineers to build up new ideas.

### 1 - Introduction

Superlattices have been conceived as man-made one-dimensional periodic structures constituted by different semiconductors for which the rather long period ( $\sim 100 \text{ \AA}$ ) would produce the subdivision of Brillouin zones into series of mini-zones (Esaki and Tsu 1969)(1). Fig. 1 shows the schematic band diagram and band structure of a  $\text{GaAs-Al}_x\text{Ga}_{1-x}\text{As}$  superlattice. Because of the existence of these mini-zones, interesting effects were predicted in these new semiconductor "crystals", in particular differential negative resistance and Bloch oscillations. In fact such properties have not been experimentally demonstrated. But practical realizations of superlattices by molecular beam epitaxy have revealed to physicists powerful technologies by which new classes of semiconductors based on thin films, can be tailored. Multiple quantum wells (MQW)(2) modulation-doped superlattices (3), and superlattice photo-avalanche structure (4)... are some of these multilayer structures. Electron devices (laser diode, field effect transistor, photo detector) made with these structures have shown excellent performances. The objective of this review is to describe these devices and to show how they are related to the concept of periodic superlattice.

### 2 - Multiple quantum wells and laser diodes

Instead of considering a superlattice as a periodic structure giving rise to interesting transport properties, DINGLE et al (2) treated the thin multilayer structures as a multiple potential well. Fig. 2 shows the wells formed by GaAs layers whereas barriers are due to  $\text{Al}_x\text{Ga}_{1-x}\text{As}$ , the larger band gap material. If the width  $L_z$  of the potential well is short as compared to the electron (or hole) de Broglie wavelength, the energies of electrons (or hole) are quantized in two-dimensional bands whose energy levels are given by

$$E = E_{//} + E_n \quad E_n = \frac{h^2}{2m} \left( \frac{n\pi}{L_z} \right)^2 \quad n = 1, 2, 3...$$

where  $E_{//}$  is the energy associated with motion in the x-y plane,  $E_z$  is the energy associated with quantization in the z direction, of the  $n^{\text{th}}$  level,  $h$  the Plank constant,  $m$  the effective mass of electron (or hole).

The two-dimensional character of the well also modifies the density of states which changes from a parabolic variation to a stepped variation as represented in Fig. 2.

The two properties - quantized subbands and step-like density of states - lead to important applications in laser diodes. As a matter of fact, the quantization of energy levels in quantum wells (QW) gives rise to transitions between subbands with the selection rule  $\Delta n = 0$ , as noted by DINGLE (5). These transitions have been experimentally observed for the first time by absorption measurements (2). Referring to fig. 2, one can immediately deduce that the transition energies in QW are higher than in bulk GaAs; therefore the wavelength associated with these transitions are shorter. Application in the domain of visible laser is evident. By using GaAs- $\text{Al}_x\text{Ga}_{1-x}\text{As}$  MQW as active layer of double heterostructure lasers CAMRAS et al (6) have fabricated visible lasers with a wavelength as short as 6500 Å. Conventional lasers with AlGaAs as active layer can work down to 7150 Å but

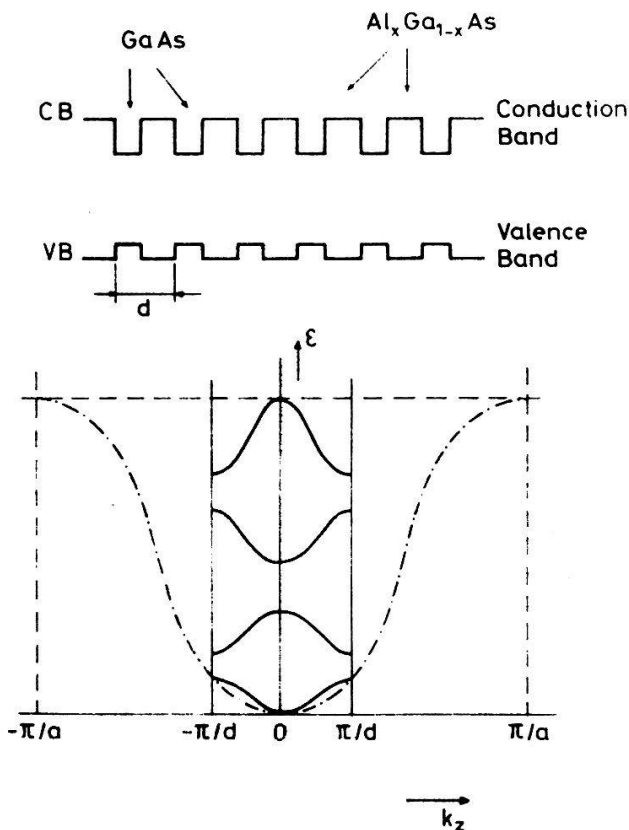


Fig. 1 Schematic band diagram and band structure of a GaAs- $\text{Al}_x\text{Ga}_{1-x}\text{As}$  periodic superlattice

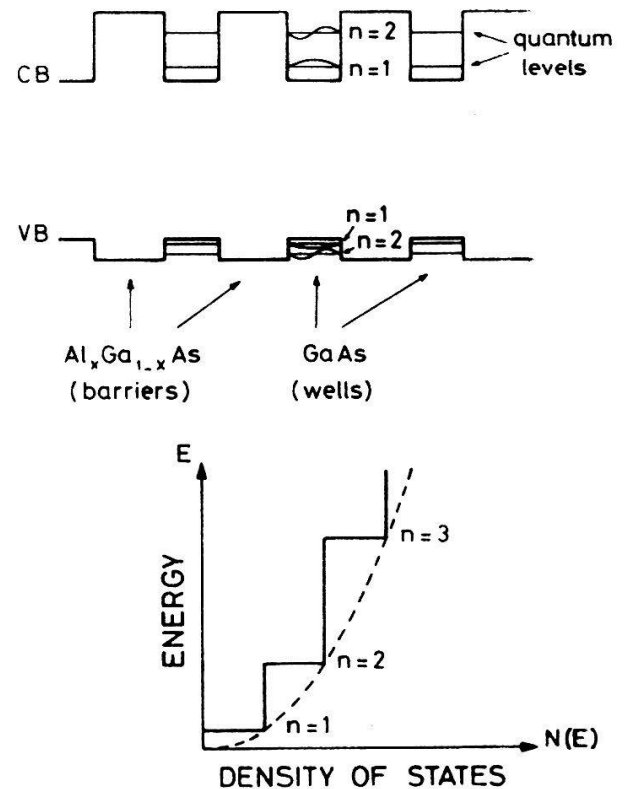


Fig. 2 GaAs- $\text{Al}_x\text{Ga}_{1-x}\text{As}$  multiple quantum well structure. The step-like density of states is characteristic of a two-dimensional system

their characteristics (CW operation, output power...) are poorer than those of MQW lasers. It was believed that part of the improved performance could be attributed to quantum size effects.

However, the interest of QW laser is certainly not limited to the realization of short wavelength laser. The step like density of states of a QW can also be used to improve the threshold current of a laser.

The first experimental evidence of the threshold current  $J_{th}$  reduction in QW laser was observed by TSANG in 1981 (7). Fig. 3 represents the schematic band diagram of the MQW laser realized by TSANG and compares it to that of a conventional laser. The improvement in  $J_{th}$  (250 A/cm<sup>2</sup> with respect to 500 A/cm<sup>2</sup> for the best conventional laser), which results from many efforts of research on superlattice (since 1969) and MQW (since 1974) is a success of a long term research programme. Better results have now been obtained with single QW lasers in which the well is positionned in a graded-refractive-index (GRIN) separate-confinement-heterostructure (SCH) (8, 9). GRIN-SCH-QW lasers offer a threshold current density as low as 121 A/cm<sup>2</sup> (9) or a threshold current of 2.5 mA (8). The latter value is 3 times lower than in conventional lasers and is the lowest ever reported.

The two-dimensional character of the QW also improves the temperature sensitivity of the laser (10, 11).

### 3 - Modulation-doped superlattices and field effect transistors

Modulation-doped superlattices are multilayer structures (for example GaAs-Al<sub>x</sub>Ga<sub>1-x</sub>As) in which the smaller band gap semiconductor layers are undoped and the larger band gap ones are n-doped (3). If the electron affinity of the smaller band gap material is higher than that of the larger band gap material (which is the case for GaAs and Al<sub>x</sub>Ga<sub>1-x</sub>As) electrons are shifted towards the smaller gap semiconductor leaving the parent donor impurities in the larger gap semiconductor. Electrons are therefore spatially separated from ionized impurities. Fig. 4 represents the schematic band diagram of a modulation-doped superlattice. Because of the charge separation, some band bending is observed both sides of the heterojunction.

The electron-impurity spatial separation is a new concept in semiconductors, since up to now the doping of semiconductors supplies both free electrons and ionized impurities in the same material. The spatial separation of electrons and impurities reduces their coulombian scattering and therefore enhances the electron mobility, particularly at low temperature where phonon scattering is reduced. DINGLE et al (3) observed for the first time, mobilities of 6000 and 20.000 cm<sup>2</sup>v<sup>-1</sup>s<sup>-1</sup> respectively at 300 and 4 K, for modulation-doped superlattices doped to the range of 10<sup>17</sup>-10<sup>18</sup>cm<sup>-3</sup>. Notice that the word "superlattice" is used here while no periodicity is required.

In fact, the notion of electron-impurity spacial separation is not limited to multilayers. Selectively-doped single heterojunctions in which GaAs is undoped and Al<sub>x</sub>Ga<sub>1-x</sub>As is n-doped also present the reduced coulombian scattering and therefore an enhancement in electron mobility. To increase the spatial separation of charges, an undoped Al<sub>x</sub>Ga<sub>1-x</sub>As spacer layer can be

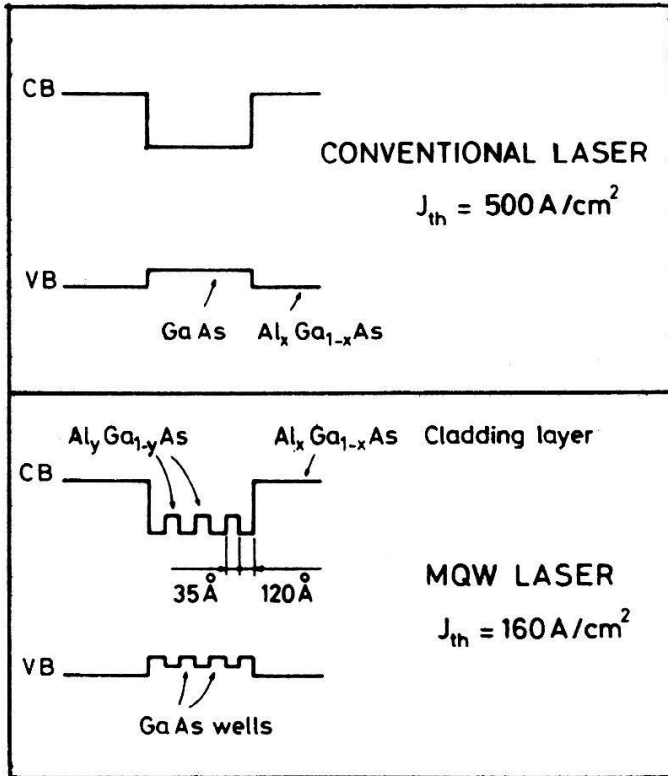


Fig. 3 Multiple quantum well lasers present lower threshold current than conventional one.

grown between the undoped GaAs and the n-doped  $\text{Al}_x\text{Ga}_{1-x}\text{As}$  layers. The thickness of the spacer layer can vary between 20 and 200 Å. Fig. 5 schematically represents a selectively-doped single heterojunction with a spacer layer and the shape of the conduction band. The interface QW can be described as a triangular potential well (12), therefore the longitudinal quantized energies are well approximated by

$$E_n = \left( \frac{\hbar^2}{2m} \right)^{1/2} \left( \frac{3}{2} \pi q \epsilon \right)^{2/3} \left( n + \frac{3}{4} \right)^{2/3}$$

$$n = 0, 1, 2, \dots$$

where  $\epsilon$  is the electric field at the interface. Because of the high electron mobility and the quantization effect in the direction perpendicular to the interface, electrons which are located in the GaAs QW are said to form a two-dimensional electron gas (2DEG).

By improving the material quality and using a thick spacer layer, several workers have obtained mobilities as high as  $10^6$ – $2 \times 10^6 \text{ cm}^2 \text{ V}^{-1} \text{ s}^{-1}$  at 4 K (13,14), in good agreement with theoretical predictions (15, 16).

The extremely high mobility achieved with the 2DEG, has led to interesting studies at high magnetic field and low temperature. The quantum Hall effect is one these studies.

Under a magnetic field perpendicular to the heterojunction interface, the 2DEG energy is quantized in discrete levels (Landau levels) which correspond to the change of density of states from a constant value to spikes, which are broadened by scattering. In a Hall experiment under high magnetic field, the electrical conductivity is determined by the position of the Fermi level in relation to the Landau subbands. When a subband is half-filled, the diagonal conductivity  $\sigma_{xx}$  is maximum. When a subband is completely filled, the gap between empty and filled Landau subbands prevents scattering from occurring and the density of states at the Fermi level tends to vanish, so that  $\sigma_{xx}$  is equal to zero at  $T = 0$ . But unlike an insulator, the off-diagonal Hall conductivity  $\sigma_{xy}$  presents

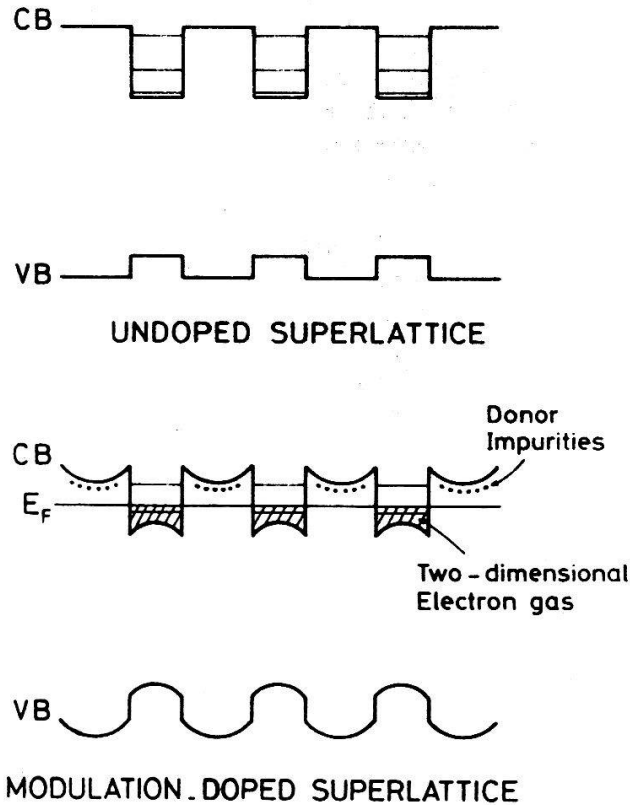


Fig. 4 Band structure of modulation superlattice

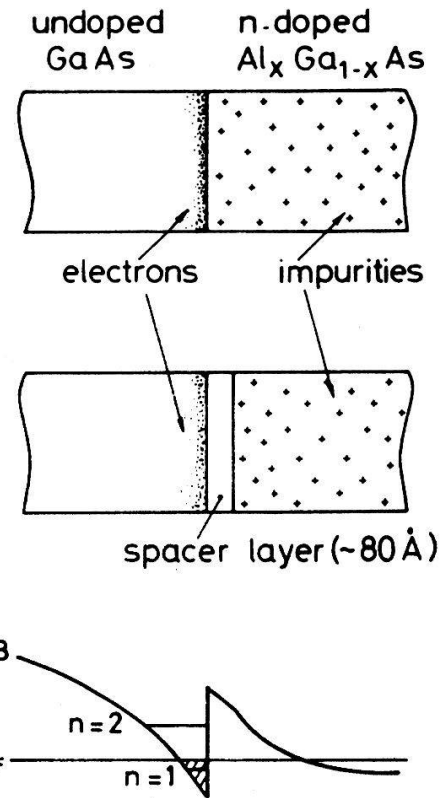


Fig. 5 Selectively doped single heterojunction

discrete values.

$$\sigma_{xy} = \frac{nq}{B} = \frac{iq^2}{h}$$

where  $n$  is the electron density and  $i$  the number of filled Landau levels. With  $\sigma_{xx} = 0$  and  $\sigma_{xy} = 0$ , the diagonal resistivity  $\rho_{xx}$  also vanishes, and the 2DEG is in a zero resistance state. While  $\rho_{xx}$  is vanishing, the off-diagonal resistivity  $\rho_{xy}$  presents plateaus with  $\rho_{xy} = h/ie^2 = \alpha^{-1} \mu_0 c/2i$  where  $\alpha$  is the fine structure constant,  $\mu_0$  the vacuum permeability and  $c$  the velocity of light. Selectively-doped heterojunctions have permitted a high precision determination of  $\rho_{xy}$ , therefore of  $\alpha$ . According to Tsui et al (17) a fantastic precision of 0.17 ppm has been obtained

$$\alpha^{-1} = 137.035968(23)$$

This determination of  $\alpha$  is the first application of the modulation doped superlattice; but the main application concerns the fabrication of field effect transistors.

The reduction of coulombian scattering in the modulation-doped 2DEG which gives rise to extremely high mobility and high electron velocity has led to the idea that transistors working with this 2DEG would present high speed and high cut-off frequency. This transistor was labelled



high electron mobility transistor (HEMT) (18) or two-dimensional electron gas field effect transistor (TEGFET) (19). The cross-sectional view of a conventional GaAs FET and a TEGFET is represented in fig. 6. Both of them use a Schottky gate to control the drain current.

Low noise TEGFETs were first fabricated by Laviron et al (19) who obtained at 10 GHz a noise figure of 2.3 dB with an associated gain of 10.2 dB. These characteristics compare favourably to GaAs FET having the same geometry (gate length  $0.8\mu\text{m}$ , unrecessed gate structure) since the latter presents 3.2dB noise figure and 8dB associated gain. TEGFETs with  $0.5\mu\text{m}$  gate length exhibit at 10 GHz, noise figures of 1.6dB (20) and 1.3dB (21). An equivalent GaAs FET, having the same parasitic elements (mainly gate and source resistances) would present a noise figure of 2.5dB. An improvement in noise figure of 1dB at 10 GHz is an impressive progress. The improvement of these microwave characteristics can be attributed to:

- the enhancement of electron velocity due to the reduced coulombian scattering and the enhanced screening effect,
- the fact that electrons in the 2DEG are located in a deep potential well, unlike the case of the GaAs FET. Because electrons in the potential well cannot be easily injected out of the well, TEGFETs present low output conductance and therefore high gain.

The enhancement of electron velocity also improves the propagation delay time of an integrated circuit. The first TEGFET integrated circuit fabricated by Mimura et al (18) exhibited a propagation delay time of 56.5 ps at 300 K and 17.1 ps at 77 K. The improvement by a factor of 3.3 between room temperature and 77K is the consequence of the enhancement of mobility and velocity of the 2DEG at low temperature. By using a gate length of  $0.7\mu\text{m}$  Tung et al (22) observed at room temperature a propagation delay time as low as 18.4 ps and a power dissipation of 0.9 mW. The same circuit can operate at 32.5 ps with 62  $\mu\text{W}$ . These values represent the best figures of merit reported so far on integrated circuits working at 300 K. They are approaching those of Josephson junction devices. In fig. 7 are reported the power-delay characteristics of the highest performance devices. It can be noted that TEGFETs are not only faster than conventional GaAs FETs, but also they have a smaller power dissipation. This latter property is an important parameter in very large scale

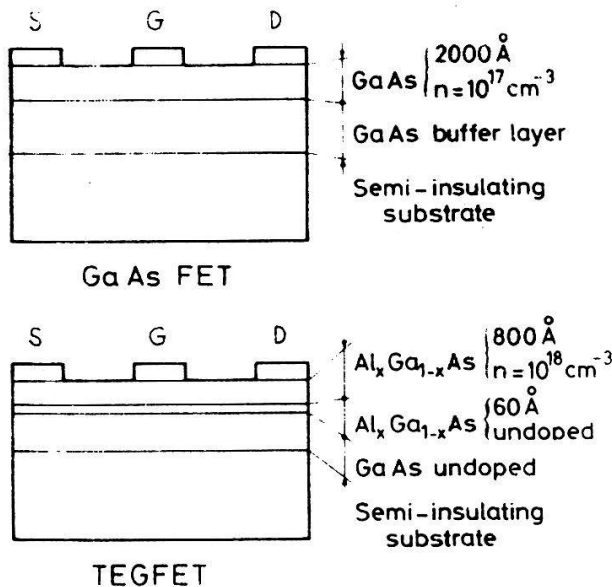


Fig. 6 Schematic cross-sectional view of a conventional GaAs FET and a two-dimensional electron gas FET.

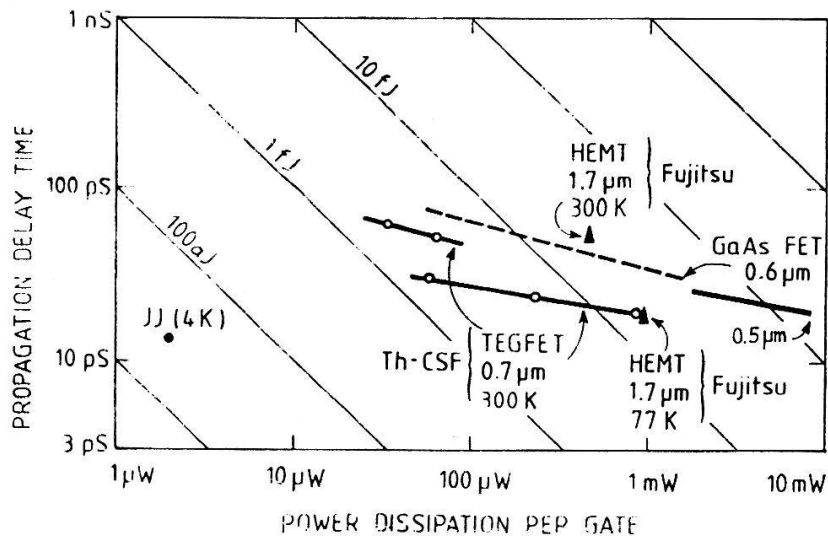


Fig. 7 TEGFET is faster and consumes less power than conventional GaAs FET

integration (VLSI) where power dissipation can represent a limiting factor.

#### 4 - Superlattice and avalanche photodiodes

A large difference between the ionization coefficient for electrons and holes is an essential requirement for low noise avalanche photodiode (APD). It is well known that in bulk GaAs, the ionization coefficients for electrons and holes are approximately equal. The utilization of a GaAs-Al<sub>x</sub>Ga<sub>1-x</sub>As multilayer can change the effective impact ionization rates for electrons and holes (4). Fig. 8 shows the band diagram of a GaAs-Al<sub>x</sub>Ga<sub>1-x</sub>As superlattice APD under bias. Whenever an electron crosses an Al<sub>x</sub>Ga<sub>1-x</sub>As-GaAs interface it gains an energy  $\Delta E_c$  corresponding to the conduction band discontinuity. At the interface holes have their energy increased by  $\Delta E_v$ . Because of the large difference between  $\Delta E_c$  and  $\Delta E_v$  ( $\Delta E_c/\Delta E_v = 4$ ) electrons gain more energy than holes. Then their impact ionization rate is becoming higher. Experiments confirm this consideration and a ratio of impact ionization rate  $\alpha/\beta$  of 10 has been measured on superlattice APD (4).

Similar effect can be obtained with a staircase structure in which graded gap multilayer structures, are used.

#### 5 - Conclusion

The three examples treated above, show that ideas are moving from the concept of a man-made periodic structure to thin multilayers in which combination of heterojunctions gives rise to new electronic properties. These properties - two-dimensional behaviour of QW, high mobility and electron velocity in selectively doped heterojunction and large impact ionization ratio  $\alpha/\beta$  in superlattice APD - lead to the fabrication of high performance electron devices which will be used in modern electronic systems : optical fiber communication for QW lasers and superlattice APD, radar links, satellite communication and supercomputer for TEGFETs.



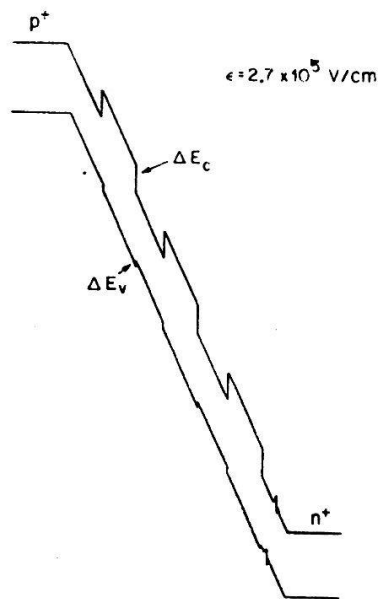


Fig. 8 : band diagram of a superlattice APD under bias

But the superlattice family is not limited to these three cited examples. This short review cannot give more details about other very interesting multilayer structures such as nipi superlattices (23), real space transfer device (24), strained superlattices (25) etc...

A tight cooperation between physicists and engineers will burst out new ideas on both fundamental solid state physics and electronic applications.

#### Acknowledgement :

Stimulating discussions with B. de Cremoux are appreciated. The author would like to thank F. Capasso for the permission to reproduce a figure from his publication.

#### References :

- (1) L. ESAKI and R. TSU IBM Res. Int. Report RC 2418 March 26 (1969)
- (2) R. DINGLE, W. WIEGMANN and C. HENRY Phys. Rev. Lett. 33, 827 (1974)
- (3) R. DINGLE, H.L. STORMER, A.C. GOSSARD and W. WIEGMANN Appl. Phys. Lett. 33, 665 (1978)
- (4) F. CAPASSO, W.T. TSANG, A.L. HUTCHINSON and G.F. WILLIAMS Appl. Phys. Lett. 40, 38 (1982)

- (5) R. DINGLE Festkörper Probleme XV. Advances in Solid State Phys. Pergamon 1975 p. 21
- (6) M.D. CAMRAS, N. HOLONYAK, K. HESS, J.J. COLEMAN, R.D. BURNHAM and D.R. SCIFRES Appl. Phys. lett. 41, 317 (1982)
- (7) W.T. TSANG Appl. Phys. lett. 39, 786 (1981)
- (8) W.T. TSANG, R.A. LOGAN and J.A. DITZENBERGER Electron. lett. 18, 845 (1982)
- (9) S.D. HERSEE, M. BALDY, P. ASSENAT, B. de CREMOUX and J.P. DUCHEMIN Electron. lett. 18, 870 (1982)
- (10) K. HESS, B.A. VOJAK, N. HOLONYAK, R. CHIN and P.D. DAPKUS Soli. State Electron. 23, 585 (1980)
- (11) Y. ARAKAWA and H. SAKAKI Appl. Phys. lett. 40, 939 (1982)
- (12) D. DELAGEBEAUEUF and N.T. LINH IEEE Trans. Electron. Dev. ED-29 955 (1982)
- (13) S. HIYAMIZU 2<sup>nd</sup> Internat. Symp. MBE and CSI Tokyo August 1982
- (14) J.C.M. HWANG, H. TEMKIN, A. KASTALSKY, H.L. STORMER and V.G. KERAMIDAS U.S. MBE workshop Oct. 1982
- (15) G. BASTARD and E.E. MENDEZ private communication
- (16) G. FISHMAN and D. CALECKI Proceed 16<sup>th</sup> Int. Conf. Phys. Semicond. "Physica 117B & 118B" p. 744 1983 North-Holland
- (17) D.C. TSUI, A.C. GOSSARD, B.F. FIELD, M.E. CAGE and R.F. DZUIBA Phys. Rev. lett. 48, 3 (1982)
- (18) T. MIMURA, K. JOSHIN, S. HIYAMIZU, K. HIKOSAKA and M. ABE Jpn J. Appl. Phys. 20, L 598 (1981)
- (19) M. LAVIRON, D. DELAGEBEAUEUF, P. DELESCLUSE, J. CHAPLART and N.T. LINH Electron. lett. 17, 536 (1981)
- (20) N. NIORI, T. SAITO, S. JOSHIN and T. MIMURA Internat. Solid State Circuit Conf. 1983
- (21) M. LAVIRON, P. DELESCLUSE, D. DELAGEBEAUEUF and N.T. LINH unpublished
- (22) P.N. TUNG, P. DELESCLUSE, D. DELAGEBEAUEUF, M. LAVIRON, J. CHAPLART and N.T. LINH Electron. lett. 18, 517 (1982)
- (23) G.H. DOHLER Phys. Stat. sol. (b) 52, 533 (1972)

- (24) K. HESS, H. MORKOC, H. SHICHIJO and B.G. STREETMAN Appl. Phys. lett. 35, 469 (1979)
- (25) G.C. OSBOURN J. Appl. Phys. 53, 1586 (1982).